Lowest Excited Triplet State of Naphthalene by Transient Polarized Resonance Raman, Matrix-Isolation Infrared, and Density-Functional-Theory Methods

Munetaka Nakata,* Satoshi Kudoh, and Masao Takayanagi

Graduate School of BASE (Bio-Applications and Systems Engineering), Tokyo University of Agriculture and Technology, 2-24-16 Naka-cho, Koganei, Tokyo 184-8588, Japan

Taka-aki Ishibashi

Surface Chemistry Laboratory, Kanagawa Academy of Science and Technology, 3-2-1 Sakato, Takatsu-ku, Kawasaki 213-0012, Japan

Chihiro Kato

Kanagawa Industrial Technology Research Institute, 705-1 Shimoimaizumi, Ebina, Kanagawa 243-0435, Japan

Received: August 10, 2000; In Final Form: September 26, 2000

Transient polarized resonance Raman spectra of naphthalene and its fully deuterated species in the lowest excited triplet state were measured. An analysis of the depolarization ratios showed that all the observed bands were assignable to the a_g vibrational modes. Matrix-isolation infrared spectra of the excited state [*J. Mol. Struct.* **1999**, *475*, 253] were remeasured to observe further bands with weak intensities. The DFT (density functional theory) calculation was also performed to confirm the vibrational assignments, where the 6-31G* basis set was used to optimize the geometrical structure. The DFT calculation is found to be useful to predict the vibrational wavenumbers of the lowest excited triplet state as well as the ground singlet state of this molecule.

Introduction

Recently we reported the matrix-isolation infrared spectra of naphthalene in the lowest excited triplet, T_1, state.[1] Ten bands of the normal ($C_{10}H_8$) and four bands of the fully deuterated ($C_{10}D_8$) species were assigned by a comparison of the observed wavenumbers with the calculated values obtained by the ab initio calculation, CIS, where configuration-interaction-singles wave function is used to compute the analytic first derivative of the energy efficiently.[2] It seemed that the calculated infrared bands agreed with the observed values within 25 cm^{-1}. On the other hand, the CIS method could not reproduce the reported Raman bands satisfactorily, where the maximum deviation was about 100 cm^{-1}. To explain this discrepancy, we proposed the possibility that some of the observed transient Raman bands are assigned to the b_{3g} vibrational mode.[1] However, this problem still remains ambiguous.

In the present study, we have measured the transient polarized resonance Raman spectra and depolarization ratios of the observed bands in order to make the vibrational assignments of the T_1 state more reasonable. We have also remeasured the infrared spectra of the transient species to observe more bands with weak intensities than those in our previous study.[1] Instead of the ab initio calculation, CIS, we have performed the DFT (density functional theory) calculation to predict the vibrational wavenumbers.

The CIS calculation method is used widely in recent years to calculate the vibrational wavenumbers of the electronically excited singlet and triplet states of various simple molecules.[3−13] On the other hand, fewer applications of the DFT calculation to triplet states have so far been published,[13−17] although this method was established as one of the best ways to predict vibrational wavenumbers of ground electronic states. For example, Mohandas and Umapathy[13] calculated the vibrational wavenumbers of *p*-benzoquinone in the T_1 state by the DFT calculation and assigned 5 and 3 bands for the normal and fully deuterated species, respectively. Hrusak et al.[16] calculated the vibrational wavenumbers of phenyl cation in the triplet state ($^3B_1$) by the DFT/B3LYP/cc-pVDZ method to interpret the experimental photoelectron spectra. In the present study, we examine the results of the DFT and CIS calculations on the T_1 state of naphthalene by a comparison with the observed vibrational bands.

Experimental and Calculation Methods

Transient Polarized Resonance Raman Spectroscopy. Samples of $C_{10}H_8$ and $C_{10}D_8$ species, purchased from Kanto Chemical Co. and Isotec Inc. (>99 at. % D) respectively, were dissolved in cyclohexane (HPLC grade, Junsei Chemical Co.) to a concentration of 10 mM. The transient polarized resonance Raman spectra were measured with the pump−probe method. The apparatus used was based on two Q-switched Nd:YAG lasers (Spectron SL801, 50 Hz, 10 ns pulse duration; Spectron SL804, 50 Hz, 17 ns pulse duration). The time interval between these lasers was controlled by a delay generator (Stanford Research Systems DG535). The fourth harmonic (266 nm, 1 mJ/pulse) of the Nd:YAG laser (SL804) was used as a pump laser to excite naphthalene molecules. A first Stokes line (416 nm, 0.6 mJ/pulse) of the H_2 Raman shifter (homemade) induced

* Corresponding author. E-mail: necom@cc.tuat.ac.jp. Tel: +81-42-388-7349. Fax: +81-42-388-7349.

10.1021/jp002924e CCC: $19.00
Published on Web 11/11/2000

by the third harmonic of the Nd:YAG laser (SL801) was used as a Raman probe laser.

The pump and probe laser beams were focused onto a thin jet-flow of the sample solution ejected from a dye laser nozzle. The Raman scattered light at right angle to the laser beams was collected and imaged through an analyzing polarizer (Polaroid sheet polarizer) and depolarizer (Babinet compensator) on the entrance slit of a triple polychromator (Jobin-Yvon T64000) with 1800 groove/mm holographic gratings. The probe laser polarization was set to be perpendicular to the scattering plane using a Glan-Taylor polarizing prism, while the analyzing polarizer was set on a computer-controlled rotating stage. The solid angle of the cone of scattered light accepted by the polychromator was about 0.1 π radian. The dispersed Raman light was detected by an intensified photodiode array detector (Princeton Instruments IRY-1024G/RB). Since the detector had no wide enough range, higher- and lower-wavenumber spectra were measured separately. Parallel and perpendicular components of Raman scattering were alternately measured 12 times and averaged to remove long-term fluctuations of the pump and probe lasers in measurements of the depolarization ratios.

Matrix-Isolation Infrared Spectroscopy. To reduce extra photoproducts and measure as many transient infrared bands as possible at a low-noise level, the sample with a mixing ratio of naphthalene/argon of about 1/5000 was prepared; it was half the concentration used previously.[1] A superhigh-pressure mercury lamp was used to increase the population of the T_1 state. A water filter was placed between the mercury lamp and the sample chamber to avoid thermal reactions. The UV light and the infrared beam of the spectrophotometer crossed each other at 45° at the matrix sample. Infrared spectra were taken at a resolution of 0.5 cm^{-1} and accumulated 64 times with an FTIR spectrophotometer. Other experimental details are shown in our previous paper.[1]

DFT Calculations. The DFT calculations were performed using the GAUSSIAN 98 program[18] with the 6-31G* basis set, employing open shell wave functions. The exchange functional used were the local spin density exchange functional of Slater[19] and the gradient corrected functional of Becke,[20] where the hybrid density functional,[21] in combination with the Lee, Yang, and Parr correlation functional (B3LYP),[22] was used to optimize the geometrical structures. The Cartesian displacements were drawn using the MolStudio R 2.0 program (NEC Co.). Details of the CIS calculations are reported elsewhere.[1]

Results

Transient Polarized Resonance Raman Spectra. The observed transient polarized resonance Raman spectra were disturbed by some strong bands due to the solvent, cyclohexane. Then, we tried to subtract the solvent bands from the observed spectra by using the spectra measured without the pumping laser light. However, it failed probably because naphthalene molecules excited by the lasers dispersed the thermal energy in surrounding solvents during measurements of the transient polarized resonance Raman spectra, resulting in band broadening of the solvents. Therefore, we subtracted the $C_{10}D_8$ spectrum from the $C_{10}H_8$ in order to cancel the solvent bands smoothly. The obtained difference spectra are shown in Figures 1 and 2 being with 10 times magnification. The high- and low-wavenumber spectra are connected after scaling so as to make the peak intensities of the bands appearing in the overlapping region nearly constant. The bands of naphthalene in the S_0 state, the intensities of which were much smaller than those of the solvent, were also subtracted. The upward and downward bands are due to the T_1 states of the $C_{10}H_8$ and $C_{10}D_8$ species, respectively. The observed wavenumbers are summarized in Table 1. Intensities of the bands in the parallel polarized spectra seemed to be stronger than those in the perpendicular polarized spectra as shown in Figures 1 and 2. The depolarization ratios, which

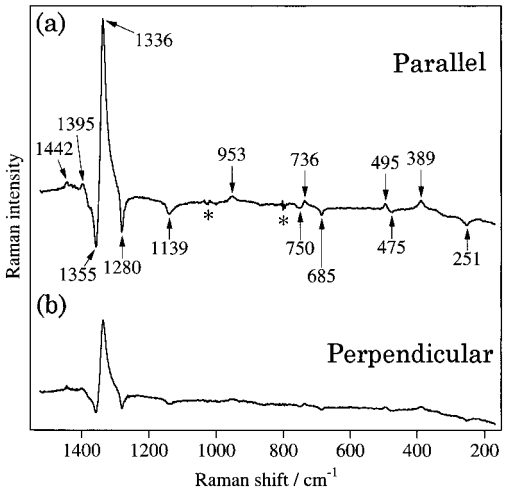

Figure 1. Differences of transient polarized resonance Raman spectra between $C_{10}H_8$ and $C_{10}D_8$: (a) parallel polarized; (b) perpendicular polarized. Upward and downward are due to $C_{10}H_8$ and $C_{10}D_8$, respectively. Bands marked by "*" are due to solvents.

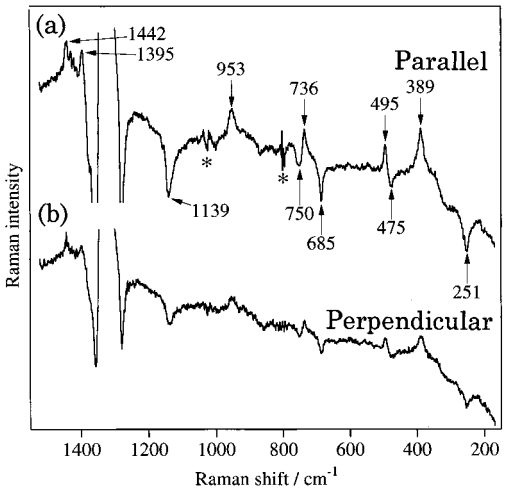

Figure 2. Drawing of Figure 1 with ten times magnification.

TABLE 1: Vibrational Wavenumbers (cm^{-1}) and Depolarization Ratios of Transient Resonance Raman Bands of Naphthalene

$C_{10}H_8$				$C_{10}D_8$			
present work		Fisher & Tripathi[c]	Takemura et al.[d]	present work		Fisher & Tripathi[c]	Takemura et al.[d]
ν^a	dep[b]			ν^a	dep[b]		
1442	0.42	1440(?)					1490
1395	0.36	1395					
1336	0.42	1337	1327	1355	0.41	1356	1343
				1280	0.40	1281	1266
			1163	1139	0.39	1142	1137
				1005[e]	?	1005	
953	0.42	958					853
				750	0.50	754	
736	0.38	741	730	685	0.44	690	664
495	0.39	496		475	0.48	476	
389	0.35	393		251	0.41		

[a] Observed wavenumbers. [b] Observed depolarization ratios. [c] In cyclohexane at room temperature.[28] [d] In 2-methylpentane glass at 77 K.[29] [e] Overlapped with solvent bands.

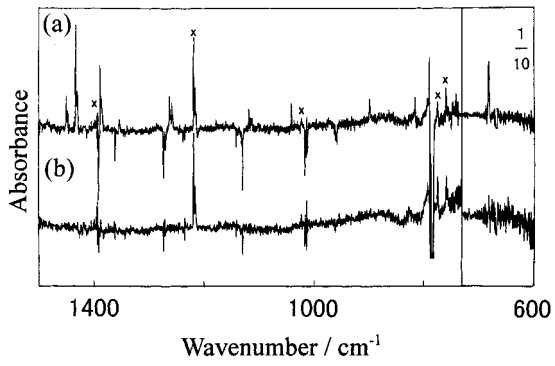

Figure 3. Matrix-isolation infrared spectra of $C_{10}H_8$: (a) difference spectrum between those measured before and during irradiation; (b) difference spectrum between those before and after irradiation. Bands marked by "X" are due to naphthalene radical cation.[23−26] The low-wavenumber region is one-tenth scaled down.

represent the ratios of intensities of parallel and perpendicular polarized spectra, are listed in Table 1. All the observed band are found to belong to the a_g vibrational modes, since the depolarization ratios are less than 0.50. To confirm this finding, we examined the depolarization ratios of some bands with b_{3g} mode for cyclohexane by the same experimental method and obtained 0.75.

Matrix-Isolation Infrared Spectra. Infrared spectra of naphthalene in low-temperature argon matrices were remeasured by a standard technique. After the measurement, we radiated UV light on the matrix sample in order to increase the population of the T_1 state. Figure 3 shows difference spectra between those measured before and during UV irradiation. The decreasing bands in (a) are assigned to the S_0 state and the increasing bands to the T_1 state or a photoproduct. The increasing bands in Figure 3b with symbol "X", 1401, 1218, 1023, 775, and 758 cm^{-1}, measured before and after irradiation, are assigned to a photoproduct produced irreversibly by UV irradiation. They agree with those of naphthalene radical cation,[23−26] 1401, 1218, 1023, 759 cm^{-1}, except for 775 cm^{-1}. It was thus considered that the radical cation was easily produced by multiphotoexcitation because the lifetimes of the electronically excited states of naphthalene in low-temperature argon matrices were expected to be longer than those in EPA solution at 77 K, 0.3 μs and 3 s for fluorescence and phosphorescence, respectively.[27] By a comparison of Figure 3a,b, we found the transient infrared bands appearing during the irradiation, where the 1354, 897, and 815 cm^{-1} bands were not reported in our previous paper.[1] The observed wavenumbers and relative intensities are summarized in Table 2.

Infrared spectra of the $C_{10}D_8$ species in an argon matrix were also measured by the same experimental method. Figure 4a,b show difference spectra between those measured before and during UV irradiation and between those before and after UV irradiation, respectively. The fully deuterated naphthalene radical cation bands appeared at 1464, 1260, 1075, and 1063 cm^{-1} in the spectra as a photoproduct produced irreversibly by UV irradiation. The ratio of signal-to-noise was so high that the 1260 cm^{-1} band of the cation, first observed in this study, seems to correspond to the 1401 cm^{-1} band of the normal species. By a comparison of these difference spectra, 10 transient infrared bands of $C_{10}D_8$ were observed. The observed wavenumbers and relative intensities are summarized in Table 2, where six bands of the transient species were first observed in this study.

DFT Calculation. The spin contamination due to the use of unrestricted open shell methodology was found to be very low, where the maximum deviation from the actual value of $S(S+1) = 2$ was not exceeding 0.05. This finding leads to a conclusion that the DFT calculations represent the T_1 state with negligible contamination from the other multiplet states. The optimized geometry of the T_1 state obtained by the DFT calculations is compared with that obtained by the CIS calculation in Figure 5. The structures obtained by these calculations are planar and have D_{2h} symmetry. The bond angles are essentially consistent in these calculations. On the other hand, the C−H lengths defined from the DFT calculation, 1.086 or 1.087 Å, are significantly longer than those from the CIS calculation, 1.075 Å. The C(1)−C(2) length, which is equivalent to C(3)−C(4), C(5)−C(6), and C(7)−C(8), and the central C(9)−C(10) length are also longer than the corresponding C−C lengths from the CIS calculation by about 0.02 Å. The other C−C lengths are approximately equal in these calculations.

The calculated wavenumbers of the Raman and infrared active modes are summarized in Tables 3 and 4, respectively, where scaling factors of 0.90 and 0.96 were used for the CIS and DFT, respectively. The depolarization ratios and relative infrared intensities obtained by the DFT method are also listed in Tables 3 and 4, respectively.

TABLE 2: Vibrational Wavenumbers (cm^{-1}) and Relative Intensities of Transient Infrared Bands of Naphthalene

$C_{10}H_8$			$C_{10}D_8$		
present work			present work		
ν^a	int[b]	Nishikida et al.[c]	ν^a	int[b]	Clark et al.[d]
3059	3[e]				
3036	3[e]				
1450	5		1404[f,g]	2	
1433	15		1339	4	
1389	10	1387			
1354[f,g]	2		1230	15	
1262	5	1257	1106[f,g]	1	
1118	3	1113	1038[f]	1	
1041	4		861[f]	2	
897[f,g]	3		853[f]	3	
815[f]	4		806[f]	4	
790	9		719	17	
682	100	681	696	6	
		385			535

[a] Observed wavenumbers. [b] Relative intensities. [c] In viscous polyethylene at 90 K.[30] [d] In Nujol at 80 K.[31] [e] Overlapped with the bands of S_0. [f] New bands observed in this study, not reported in ref 1. [g] Not assigned to the T_1 state; see text.

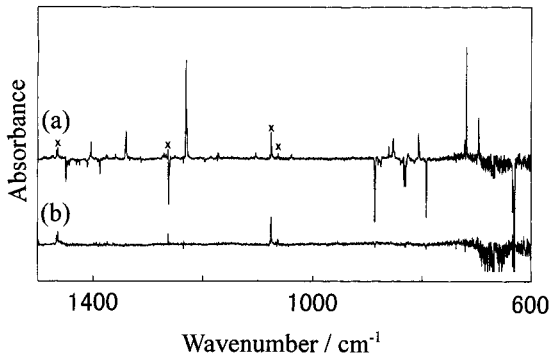

Figure 4. Matrix-isolation infrared spectra of $C_{10}D_8$: (a) difference spectrum between those measured before and during irradiation; (b) difference spectrum between those before and after irradiation. Bands marked by "X" are due to naphthalene radical cation.[26]

Discussion

Transient Resonance Raman Spectra.. *Comparison of Observed Bands with Previous Results*. The transient resonance

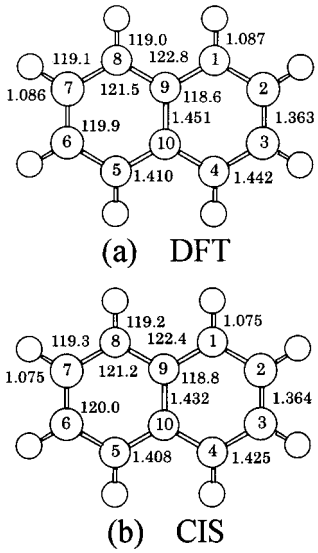

Figure 5. Optimized geometrical structures of the lowest excited triplet state of naphthalene: (a) DFT calculation; (b) CIS calculation. Bond lengths and bonded angles are given in ångstroms and degrees, respectively.

TABLE 3: Calculated Wavenumbers (cm^{-1}) and Depolarization Ratios of Raman Active Modes in the T_1 State

	$C_{10}H_8$			$C_{10}D_8$		
		DFT			DFT	
sym	CIS ν^a	ν^b	dep[c]	CIS ν^a	ν^b	dep[c]
$1a_g$	3054	3087	0.13	2263	2289	0.14
$2a_g$	3032	3065	0.64	2240	2263	0.53
$3a_g$	1536	1597	0.15	1493	1562	0.15
$4a_g$	1452	1433	0.23	1229	1275	0.54
$5a_g$	1245	1354	0.22	1303	1363	0.22
$6a_g$	1136	1145	0.65	851	854	0.23
$7a_g$	1019	1022	0.28	815	809	0.52
$8a_g$	727	727	0.10	667	666	0.10
$9a_g$	483	487	0.36	465	469	0.35
$1b_{3g}$	3037	3070	0.75	2240	2264	0.75
$2b_{3g}$	3022	3056	0.75	2227	2250	0.75
$3b_{3g}$	1408	1385	0.75	1306	1269	0.75
$4b_{3g}$	1364	1319	0.75	1178	1139	0.75
$5b_{3g}$	1187	1168	0.75	999	981	0.75
$6b_{3g}$	937	915	0.75	837	829	0.75
$7b_{3g}$	900	881	0.75	759	744	0.75
$8b_{3g}$	474	464	0.75	458	450	0.75
$1b_{2g}$	939	906	0.75	772	761	0.75
$2b_{2g}$	804	792	0.75	744	713	0.75
$3b_{2g}$	711	696	0.75	577	568	0.75
$4b_{2g}$	454	460	0.75	401	408	0.75
$1b_{1g}$	812	769	0.75	655	622	0.75
$2b_{1g}$	683	674	0.75	508	501	0.75
$3b_{1g}$	294	278	0.75	260	245	0.75

[a] Wavenumbers calculated by CIS/6-31G*. A scaling factor of 0.90 is used.[1] [b] Wavenumbers calculated by DFT/B3LYP/6-31G*. A scaling factor of 0.96 is used. [c] Depolarization ratios calculated by DFT/B3LYP/6-31G*.

Raman spectra were reported by Fisher and Tripathi[28] and Takemura et al.[29] Their results are compared with ours in Table 1. The wavenumbers of the bands in our spectra are essentially consistent with those obtained by Fisher and Tripathi but are systematically higher than those of Takemura et al. by about 20 cm^{-1} or less, probably because of the errors in wavenumber calibration. We could not confirm the 1163 cm^{-1} band of $C_{10}H_8$ and the 1490 and 853 cm^{-1} bands of $C_{10}D_8$ reported by them.[29] One band of the $C_{10}D_8$ species, first observed at 252 cm^{-1}, probably corresponds to the 389 cm^{-1} band of the $C_{10}H_8$ species.

TABLE 4: Calculated Wavenumbers (cm^{-1}) and Relative Intensities of Infrared Active Modes in the T_1 State and Assignments of the Observed Bands

	$C_{10}H_8$				$C_{10}D_8$			
		DFT				DFT		
sym	CIS ν^a	ν^b	int[c]	obs ν^d	CIS ν^a	ν^b	int[c]	obs ν^d
$1b_{1u}$	3040	3072	64.3	3036	2244	2266	42.8	
$2b_{1u}$	3026	3059	7.7		2233	2255	1.8	
$3b_{1u}$	1427	1412	8.1	1433	1335	1347	0.2	1339
$4b_{1u}$	1382	1369	7.4	1389	1208	1203	10.1	1230
$5b_{1u}$	1238	1243	7.7	1262	1038	1023	1.0	1038
$6b_{1u}$	1019	1018	<0.1	1041	847	844	<0.1	853
$7b_{1u}$	784	774	6.1	790	712	703	6.9	719
$8b_{1u}$	349	345	0.1		319	316	0.1	
$1b_{2u}$	3050	3084	66.1	3059	2260	2288	37.2	
$2b_{2u}$	3025	3059	7.3		2226	2250	5.2	
$3b_{2u}$	1465	1492	0.8		1353	1461	0.4	
$4b_{2u}$	1315	1435	3.5	1450	1249	1347	0.1	
$5b_{2u}$	1130	1161	<0.1		838	870	0.9	861
$6b_{2u}$	1054	1091	7.9	1118	833	835	7.5	806
$7b_{2u}$	777	824	<0.1		747	770	<0.1	
$8b_{2u}$	582	574	14.6		560	553	12.3	
$1b_{3u}$	831	789	5.7	815	698	672	7.7	696
$2b_{3u}$	705	674	108.2	682	553	526	49.3	535
$3b_{3u}$	401	382	5.0	385	342	324	8.5	
$4b_{3u}$	161	162	2.1		148	148	1.9	

[a] Wavenumbers calculated by CIS/6-31G*. A scaling factor of 0.90 is used.[1] [b] Wavenumbers calculated by DFT/B3LYP/6-31G*. A scaling factor of 0.96 is used. [c] Relative infrared intensity calculated by DFT/B3LYP/6-31G*. [d] Experimental wavenumbers listed in Table 2.

Comparison of Observed Bands with DFT Calculation. The wavenumbers of the $9a_g$, $8a_g$, $7a_g$, $6a_g$, $5a_g$, $4a_g$, and $3a_g$ modes for $C_{10}H_8$ are predicted to be 487, 727, 1022, 1145, 1354, 1433, and 1597 cm^{-1} by the DFT calculation. The bands observed at 495, 736, 1336, and 1442 cm^{-1} agree with the $9a_g$, $8a_g$, $5a_g$, and $4a_g$ modes, respectively, within 20 cm^{-1}. The corresponding bands for $C_{10}D_8$ are predicted to be 469, 666, 809, 854, 1363, 1275, and 1562 cm^{-1}. The bands observed at 475, 685, 1355, and 1280 cm^{-1} agree with the $9a_g$, $8a_g$, $5a_g$ and $4a_g$ modes, respectively, within 20 cm^{-1}, too. The most intense band shows an increase in the wavenumbers on deuteration from 1336 to 1355 cm^{-1}. The $5a_g$ mode, predicted by the DFT calculation, also shows an increase from 1354 to 1363 cm^{-1}. This finding supports our assignment for the most intense bands.

The 953 cm^{-1} band of $C_{10}H_8$ and the 750 cm^{-1} band of $C_{10}D_8$ are tentatively assigned to the $7a_g$ mode. They differ from the corresponding calculated values by about 70 and 60 cm^{-1}, respectively, but the observed isotope shift, 203 cm^{-1}, is consistent with that calculated, 213 cm^{-1}. Another possible assignment is the combination modes of $2b_{1g}$ and $3b_{1g}$, where the wavenumbers are calculated to be $674 + 278 = 952$ and $501 + 245 = 746$ cm^{-1} for $C_{10}H_8$ and $C_{10}D_8$, respectively. The consistency between the observed and calculated values is better than the assignments to the $7a_g$ mode. The bands of the $3a_g$ and $6a_g$ modes were not observed in the expected regions, probably because of their weak intensities or overlapping with other bands.

The 389 cm^{-1} band of $C_{10}H_8$ and the 252 cm^{-1} band of $C_{10}D_8$ still remain unassigned. These bands should be assigned to a_g modes, judging from the analysis of the depolarization ratios. However, the results of the DFT calculation showed no a_g-mode bands below 487 and 469 cm^{-1} for $C_{10}H_8$ of $C_{10}D_8$, respectively. It is also impossible to assign them to any overtone or combination modes. For example, the lowest calculated wavenumber of $C_{10}D_8$ is predicted to be 148 cm^{-1} for the $4b_{3u}$ mode and overtone of this band, 296 cm^{-1}, is much higher than the

TABLE 5: Vibrational Assignments of the Observed Raman Bands

vibrational assignments	$C_{10}H_8$		$C_{10}D_8$	
	obs	calc[a]	obs	calc[a]
$4a_g$	1442	1433	1280	1275
$5a_g$	1336	1354	1355	1363
$7a_g$	953[b]	1022	750[b]	809
$8a_g$	736	727	685	666
$9a_g$	495	487	475	469
$3b_{2g} + 3b_{2g}$	1395	1392 = 696 + 696	1139	1136 = 568 + 568
$2b_{1g} + 2b_{1g}$	c	1348 = 674 + 674	1005	1002 = 501 + 501
$2b_{1g} - 3b_{1g}$	389	396 = 674 − 278	251	256 = 501 − 245

[a] Wavenumberes calculated by DFT/B3LYP/6-31G*. A scaling factor of 0.96 is used. [b] These bands may be assigned to $2b_{1g} + 3b_{1g}$. [c] Overlapped with the $5a_g$ mode.

observed wavenumber, 252 cm^{-1}. Furthermore, the isotope shift from 389 to 252 cm^{-1} seems to be too large for vibrational modes of normal molecules. One possibility is that these bands are due to stokes lines from $3b_{1g}$ to $2b_{1g}$, where the wavenumbers are calculated to be 674−278 = 396 and 501−245 = 256 cm^{-1} for $C_{10}H_8$ and $C_{10}D_8$, respectively. Another possibility is that these low-wavenumber bands originate from clusters such as dimer or excimer. If this band is related to an intermolecular interaction through the C−H bond, a large isotope shift may be expected. However, this possibility can be ruled out by the fact that no new bands appeared in the spectra of the $C_{10}H_8$/$C_{10}D_8$ mixed sample measured by the same experimental method.

Fisher and Tripathi[28] assigned the 1139 and 1005 cm^{-1} bands of $C_{10}D_8$ to the b_{3g} mode. However, our analysis of the depolarization ratios leads to the conclusion that the 1139 cm^{-1} band is due to an a_g mode. It conflicts with the result of the DFT calculation, which showed that no a_g-mode bands exist between 854 and 1275 cm^{-1}. Therefore, we assumed that these bands, 1139 and 1005 cm^{-1}, are assigned to the overtone modes of $3b_{2g}$ and $2b_{1g}$, respectively, where the calculated values are 568 + 568 = 1136 and 501 + 501 = 1002 cm^{-1}. The band for $C_{10}H_8$ corresponding to 1139 cm^{-1} was observed at 1395 cm^{-1}, where the calculated value is 696 + 696 = 1392 cm^{-1}. The band for $C_{10}H_8$ corresponding to 1005 cm^{-1}, where the calculated value is 674 + 674 = 1348 cm^{-1}, seems to overlap with the most intense $5a_g$ mode appearing at 1336 cm^{-1}. Our assignments for the observed resonance Raman bands are summarized in Table 5.

Comparison of DFT with CIS Calculation. The calculated wavenumbers obtained by the CIS calculation are approximately equal to those by the DFT calculation. However, the wavenumbers of the most intense $5a_g$ mode of the CIS method is lower than that of the DFT method by 109 cm^{-1}. To find the origin of this discrepancy, we examined the Cartesian displacements of this mode. As drawn in Figure 6, the $5a_g$ mode is a mixture of the central C−C stretching and C−H bending modes. The direction of the C(2)−H bending, which is equivalent to the C(3)−H, C(6)−H and C(7)−H bending, of the CIS is opposite to that of the DFT. This finding means that the sign of the off-diagonal force constant between the central C−C stretching and C(2)−H bending is opposite. This is one of the reasons that the vibrational wavenumbers strongly depends on the degrees of mixing of the C−C and C−H stretching modes. Since the DFT calculation considers effects of multielectron configuration in a term of potential of Hamiltonian, but the CIS calculation considers only one-electron excited state, the DFT calculation seems to make more reasonable predictions of the vibrational wavenumbers for the lowest excited triplet state. It is found that the observed wavenumbers of this mode, 1336 cm^{-1}, is close to the result of DFT, 1354 cm^{-1}, but not of CIS, 1245 cm^{-1}.

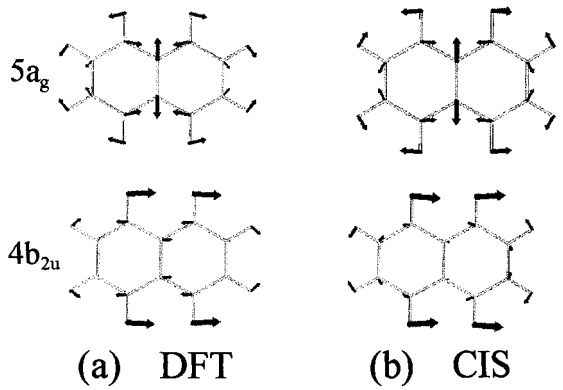

Figure 6. Cartesian displacements of $5a_g$ and $4b_{2u}$ modes: (a) DFT calculation; (b) CIS calculation.

Matrix-Isolation Infrared Spectra. *Comparison of Observed Bands with Previous Studies*. Nishikida et al.[30] reported five T_1 bands of $C_{10}H_8$ in viscous polyethylene at 90 K, while Clark et al. reported one band of $C_{10}D_8$ in Nujol at 80 K.[31] Since the range of measurement of our experimental was 600 cm^{-1} or higher, we could not confirm the 385 and 535 cm^{-1} bands for the $C_{10}H_8$ and $C_{10}D_8$ species, respectively. Other bands are essentially consistent with ours within 5 cm^{-1}, as shown in Table 2.

Comparison of Observed Bands with DFT Calculation. The calculated wavenumbers obtained by the DFT calculation are compared with the observed values in Table 4, where we assign the observed bands considering the wavenumbers and relative intensities. The wavenumbers of the bands are consistent with the calculated values within 30 cm^{-1}, except for the C−H stretching modes. It is known that a smaller scaling factor is necessary for high-wavenumber bands such as C−H stretching.[32] The weak 1354 and 897 cm^{-1} bands of $C_{10}H_8$ and 1404 and 1106 cm^{-1} bands of $C_{10}D_8$, observed first in this study, could not be assigned to the T_1 state. These bands may be assigned to other transient species but not a photoproduct, since they did not appear in Figure 2b or 3b. Further information is necessary to identify the species. Since the DFT calculation reproduces the observed wavenumbers satisfactorily for both the normal and fully deuterated species as well as the Raman active mode, we conclude that the DFT calculation can predict the wavenumbers of the lowest excited triplet state of naphthalene as well as the ground singlet state.

Comparison of DFT Calculation with CIS Calculation. The tendency seen in the Raman-active modes is also seen in the infrared active modes. The wavenumbers of the $4b_{2u}$ mode calculated by CIS is different from that calculated by DFT by 120 cm^{-1}. Like the $5a_g$ mode, the direction of the C(2)−H, C(3)−H, C(6)−H, and C(7)−H bending in the $4b_{2u}$ mode of CIS is opposite to that of DFT, as shown in Figure 6. It is certain that the band observed at 1450 cm^{-1} agree well with that estimated by DFT, 1435 cm^{-1}, but not CIS, 1315 cm^{-1}. However, one may notice that the CIS calculation agrees with the observation better than the DFT calculation, including the $C_{10}D_8$ bands, if the 1450 and 1118 cm^{-1} bands are assigned to $3b_{2u}$ and $5b_{2u}$, respectively, where the calculated values obtained by the CIS method are 1465 and 1130 cm^{-1}. Further applications of DFT to other molecules are useful to test which calculation method is more reasonable to estimate vibrational wavenumbers for the lowest excited triplet states.

Acknowledgment. The authors wish to thank Professors Kozo Kuchitsu (Josai University), Tahei Tahara (Institute for Molecular Science), and Koichi Ohno (Tohoku University) for their helpful discussions. T.I. acknowledges the receipt of a Grant-in-Aid (No. 09740455) from the Ministry of Education, Science, and Culture.

References and Notes

(1) Kudoh, S.; Takayanagi, M.; Nakata, M. *J. Mol. Struct.* **1999**, *475*, 253.
(2) Foresman, J. B.; Head-Gordon, M.; Pople, J. A. *J. Phys. Chem.* **1992**, *96*, 135.
(3) Pan, D.; Shoute, L. C. T.; Phillips, D. L. *Chem. Phys. Lett.* **1999**, *303*, 629.
(4) Raab, A.; Worth, G. A.; Meyer, H.-D.; Cederbaum, L. S. *J. Chem. Phys.* **1999**, *110*, 936.
(5) Troxyler, T. *J. Phys. Chem. A* **1998**, *102*, 4775.
(6) Tzeng, W. B.; Narayanan, K.; Shieh, K. C.; Tung, C. C. *J. Mol. Struct.* **1998**, *428*, 231.
(7) Goodpaster, J. V.; Harrison, J. F.; McGuffin, V. L. *J. Phys. Chem. A* **1998**, *102*, 3372.
(8) Becussi, M.; Lakin, N. M.; Pietraperzia, G.; Salvi, P. R.; Castellucci, E. *J. Chem. Phys.* **1997**, *107*, 10399.
(9) Tzeng, W. B.; Narayanan, K.; Hsieh, C. Y.; Tuang, C. C. *Spectrochim. Acta A* **1997**, *53*, 2595.
(10) Zgierski, M. Z. *J. Chem. Phys.* **1997**, *107*, 7732.
(11) Mebel, A. M.; Chen, Y.-T.; Lin, S.-H. *Chem. Phys. Lett.* **1997**, *275*, 19.
(12) Jas, G. S.; Kyczeram, K. *Chem. Phys.* **1997**, *214*, 229.
(13) Mohandas, P.; Umapathy, S. *J. Phys. Chem. A* **1997**, *101*, 4449.
(14) Simard, B.; Presunka, P. I.; Loock, H. P.; Berces, A.; Launila, O. *J. Chem. Phys.* **1997**, *107*, 307.
(15) Stueckl, A. C.; Daul, C. A.; Guedel, H. U. *J. Chem. Phys.* **1997**, *107*, 4606.
(16) Hrusak, J.; Schroeder, D.; Iwata, S. *J. Chem. Phys.* **1997**, *106*, 7541.
(17) Zilberg, S.; Haas, Y.; Shaik, S. *J. Phys. Chem.* **1995**, *99*, 16558.
(18) Frisch, M. J.; Trucks, G. W.; Schlegel, H. B.; Scuseria, G. E.; Robb, M. A.; Cheeseman, J. R.; Zakrzewski, V. G.; Montgomery, Jr. J. A.; Stratmann, R. E.; Burant, J. C.; Dapprich, S.; Millam, J. M.; Daniels, A. D.; Kudin, K. N.; Strain, M. C.; Farkas, O.; Tomasi, J.; Barone, V.; Cossi, M.; Cammi, R.; Mennucci, B.; Pomelli, C.; Adamo, C.; Clifford, S.; Ochterski, J.; Petersson, G. A.; Ayala, P. Y.; Cui, Q.; Morokuma, K.; Malick, D. K.; Rabuck, A. D.; Raghavachari, K.; Foresman, J. B.; Cioslowski, J.; Ortiz, J. V.; Stefanov, B. B.; Liu, G.; Liashenko, A.; Piskorz, P.; Komaromi, I.; Gomperts, R.; Martin, R. L.; Fox, D. J.; Keith, T.; Al-Laham, M. A.; Peng, C. Y.; Nanayakkara, A.; Gonzalez, C.; Challacombe, M.; Gill, P. M. W.; Johnson, B.; Chen, W.; Wong, M. W.; Andres, J. L.; Gonzalez, C.; Head-Gordon, M.; Replogle, E. S.; Pople, J. A. *Gaussian98*; Gaussian, Inc.: Pittsburgh, PA, 1998.
(19) Slater, J. C. Quantum *Theory of Molecules and Solids*; McGraw-Hill: New York, 1974; Vol. 4.
(20) Becke, A. D. *Phys. Rev. A* **1988**, *38*, 3098.
(21) Becke, A. D. *J. Chem. Phys.* **1993**, *98*, 5648.
(22) Lee, C.; Yang, W.; Parr, R. G. *Phys. Rev. B* **1988**, *37*, 785.
(23) Szczepanski, J.; Roser, D.; Personette, W.; Eyring, M.; Pellow, R.; Vala, M. *J. Phys. Chem.* **1992**, *96*, 7876.
(24) Pauzat, F.; Talbi, D.; Miller, M. D.; DeFrees, D. J.; Ellinger, Y. *J. Phys. Chem.* **1992**, *96*, 7882.
(25) Hudgins, D. M.; Sandford, S. A.; Allamandola, L. J. *J. Phys. Chem.* **1994**, *98*, 4243.
(26) Langhoff, S. R. *J. Phys. Chem.* **1996**, *100*, 2819.
(27) Becker, R. S. *Theory and interpretation of fluorescence and phosphorescence*; John Wiley & Sons: New York, 1969.
(28) Fisher, M. R.; Tripathi, G. N. R. *J. Chem. Phys.* **1985**, *82*, 4721.
(29) Takemura, T.; Fujita, M.; Baba, H. *Chem. Phys. Lett.* **1982**, *91*, 390.
(30) Nishikida, K.; Kamura, Y.; Seki, K.; Iwasaki, N.; Kinoshita, M. *Mol. Phys.* **1983**, *49*, 1505.
(31) Clarke, R. H.; Kosen, P. A.; Lowe, M. A.; Mann, R. H.; Mushlin, R. *J. Chem. Soc., Chem. Commun.* **1973**, 528.
(32) Kudoh, S.; Takayanagi, M.; Nakata, M. *J. Mol. Struct.* **2000**, *322*, 363.